

THE ONSET OF THE GEV AFTERGLOW OF GRB 090510

G. GHIRLANDA¹, G. GHISELLINI¹ AND L. NAVA^{1,2}

Draft version February 13, 2022

ABSTRACT

We study the emission of the short/hard GRB 090510 at energies > 0.1 GeV as observed by the Large Area Telescope (LAT) onboard the *Fermi* satellite. The GeV flux rises in time as t^2 and decays as $t^{-1.5}$ up to 200 s. The peak of the high energy flux is delayed by 0.2 s with respect to the main \sim MeV pulse detected by the *Fermi* Gamma Burst Monitor (GBM). Its energy spectrum is consistent with $F(\nu) \propto \nu^{-1}$. The time behavior and the spectrum of the high energy LAT flux are strong evidences of an afterglow origin. We then interpret it as synchrotron radiation produced by the forward shock of a fireball having a bulk Lorentz factor $\Gamma \sim 2000$. The afterglow peak time is independent of energy in the 0.1–30 GeV range and coincides with the arrival time of the highest energy photon (~ 30 GeV). Since the flux detected by the GBM and the LAT have different origins, the delay between these two components is not entirely due to possible violation of the Lorentz invariance. It is the LAT component by itself that allows to set a stringent lower limit on the quantum-gravity mass of 4.7 times the Planck mass.

Subject headings: Gamma rays: bursts — Radiation mechanisms: non-thermal — X-rays: general

1. INTRODUCTION

GRB 090510 is a short/hard burst at redshift $z=0.903\pm 0.003$ (Rau et al. 2009) detected by *Fermi* (Guiriec et al. 2009), AGILE (Longo et al. 2009), *Swift* (Hoversten et al. 2009), *Konus-Wind* (Golenetskii et al. 2009) and *Suzaku* (Ohmori et al. 2009).

The *Fermi*-Gamma Burst Monitor (GBM) triggered on a precursor while the main emission episode in the 8 keV–40 MeV energy range starts ~ 0.5 s after trigger and lasts up to ~ 1 s. The emission observed by the *Fermi*-Large Area Telescope (LAT) starts 0.65 s after the trigger and lasts ~ 200 s. The joint GBM-LAT spectral analysis showed the presence of two components. *Fermi*-LAT detected a 31 ± 3 GeV photon delayed by 0.829 s with respect to the trigger (Abdo et al. 2009 – A09 hereafter).

The precursor was not seen by AGILE, that triggered on the main emission episode. The flux detected by the Mini Calorimeter (MCAL, 0.3–10 MeV) lasts 0.2 s. As it ends, the Gamma Ray Imaging Detector (GRID, 0.03 – 30 GeV) starts to detect a high energy component lasting for 10 s and decaying as $t^{-1.3}$ (Giuliani et al. 2009).

The distinguishing property of GRB 090510 arising from the *Fermi* and AGILE data is that the \sim MeV emission component, commonly detected in GRBs, is followed by a much longer lasting high energy emission detected above 100 MeV. Both the AGILE and *Fermi* spectra suggest that this component is not the extrapolation of the soft \sim MeV spectrum to the GeV range. A09 interpret the \sim MeV flux as synchrotron radiation and the LAT flux as its synchrotron self-Compton emission. The detection by *Fermi* of a 30 GeV photon sets a lower limit on the bulk Lorentz factor of the fireball $\Gamma > 1000$, based on the compactness argument (A09). The 30 GeV photon arrives 0.829 s after the trigger (set by the precursor) and 0.3 s after the beginning of the GBM main pulse. These

delays allowed A09 to put limits on the violation of the Lorentz invariance.

In this paper we propose a different interpretation of the emission detected by the *Fermi*-LAT and AGILE. If $\Gamma > 1000$ the fireball should start to decelerate and produce a luminous afterglow rather early (e.g. Piran 2005), even at the sub-second timescale. By analyzing the *Fermi*-LAT light-curve and spectra we present strong evidences that the flux detected by the LAT is afterglow emission of the forward external shock. In this framework we derive the initial Γ of the fireball and set a lower limit on the quantum-gravity mass.

Recent works on the high energy emission of LAT-detected GRBs include Kumar & Barniol Duran (2009), discussing GRB 080916C (Abdo et al. 2009a). Also for this burst they proposed that the LAT-detected flux can be synchrotron produced in the external shock (see also Gao et al. 2009 for GRB 090510; see also Fan et al. 2008; Zou, Fan & Piran 2009; Zhang & Peer 2009 for an inverse Compton origin). Hadronic models have been proposed to explain the emission properties of GRB 080916C (Razzaque, Dermer & Finke 2009).

2. *Fermi*-LAT DATA ANALYSIS

We have analyzed the *Fermi*-LAT data of GRB 090510 with the *Fermi ScienceTools* (v9r15p2) released on Aug. 8th 2008. Photons were selected (with the `gtselect` tool) around RA=333.552° and Dec=−26.598°. Different energy bins were considered for the analysis of the LAT light curve but only photons with energy > 100 MeV were extracted. Light curves and spectra were created with the `gtbin` tool. The spectral response files were created with the `gtrspgen`. The spectra were analyzed with `Xspec` (v. 12).

3. RESULTS

Fig. 1 shows the light curve considering all the LAT photons with energies > 100 MeV. The times are scaled to $T^* = 0.6$ s which corresponds to the time of the first main pulse observed by the GBM. We fit the light curve

arXiv:0909.0016v1 [astro-ph.HE] 31 Aug 2009

Electronic address: giancarlo.ghirlanda@brera.inaf.it

¹ INAF-Osservatorio Astronomico di Brera, via Bianchi 46, I-23807 Merate, Italy

² Univ. dell'Insubria, V. Valleggio, 11, I-22100, Como, Italy

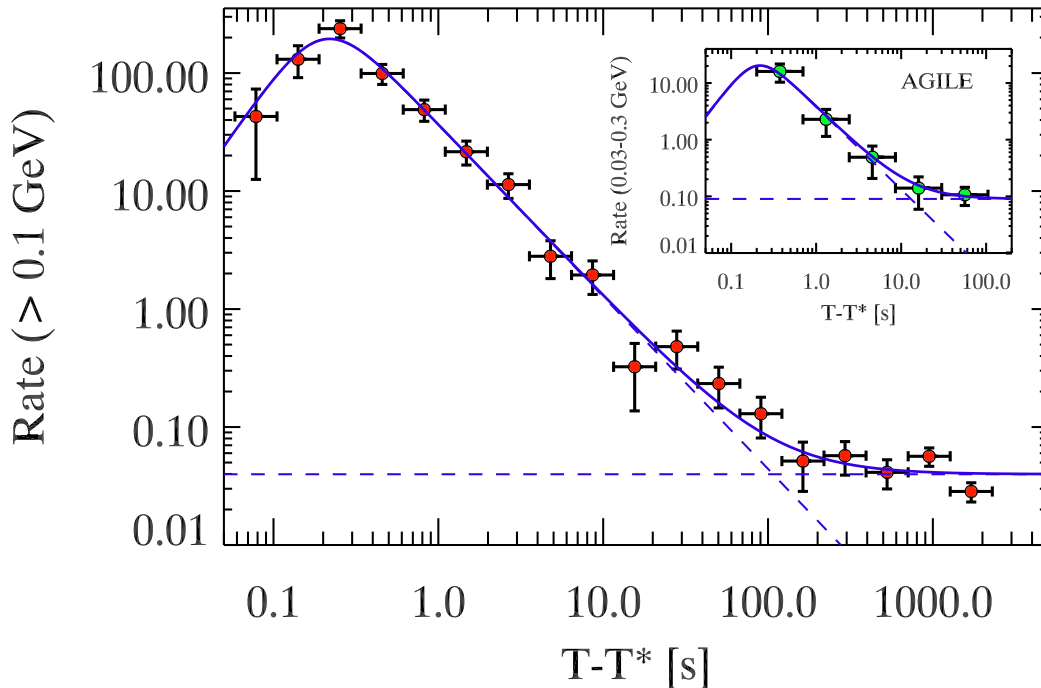


FIG. 1.— *Fermi*-LAT light curve of the emission of GRB 090510 above 100 MeV. The times were scaled to the time $T^* = 0.6$ s after the GBM trigger. This is the time corresponding to the main pulse of emission detected by the GBM in the 8 keV–10 MeV energy range (see A09). The solid line is the best fit to the data points obtained with a smoothly broken power-law plus a constant (dashed lines). The inset shows the AGILE light curve (photons energies between 30 and 300 MeV). The curve is the best fit of the *Fermi* data scaled to the AGILE data points.

with the sum of two components, i.e. a smoothly broken power-law and a constant to account for the flattening of the flux visible after 200 s:

$$R(t) = \frac{A(t/t_b)^\alpha}{1 + (t/t_b)^{\alpha+\beta}} + B \quad (1)$$

When $\alpha > 0$ and $\beta > 0$ Eq. 1 has a peak at $t_{\text{peak}} = t_b (\alpha/\beta)^{1/(\alpha+\beta)}$. The standard afterglow theory (Sari & Piran 1999) requires $\alpha = 2$. Fixing $\alpha = 2$, the best fit parameters ($\chi^2=14.6/14$) are $A = 385_{-40}^{+45}$ counts/s, $t_{\text{pk}} = 0.217 \pm 0.015$ s, $\beta = 1.46_{-0.03}^{+0.06}$ and $B = 4 \times 10^{-2}$ counts/s. The best fit is shown by the solid line in Fig. 1. The AGILE light curve (adapted from Giuliani et al. 2009) of the photons detected by the GRID between 30 MeV and 300 MeV is also shown in Fig. 1 (inset). The *Fermi* and AGILE light curves are consistent with the same decay law, i.e. $t^{-1.5}$, although AGILE missed the rising phase of the GeV emission.

The emission above 100 MeV peaks at $T - T^* = 0.22$ s (i.e. 0.82 s after the GBM trigger). The time of the peak coincides with the arrival time of the highest energy photon of 30 GeV. Fig. 1 shows that the LAT flux lasts for about 200 s (and it sets to the background level afterwards). Instead, the emission detected by the GBM in the 8 keV–10 MeV energy range ceases after ~ 1 s (A09).

Fig. 2 shows the LAT light curve in the first 10 s separated in two energy bands, i.e. 0.1–1 GeV and >1 GeV (top and middle panels, respectively). The curves correspond to the same best fit obtained from the >0.1 GeV light curve (Fig. 1), only re-normalized to the data points. We further separated the light curve into four broad energy channels: 0.1–0.2 GeV, 0.2–0.4 GeV, 0.4–

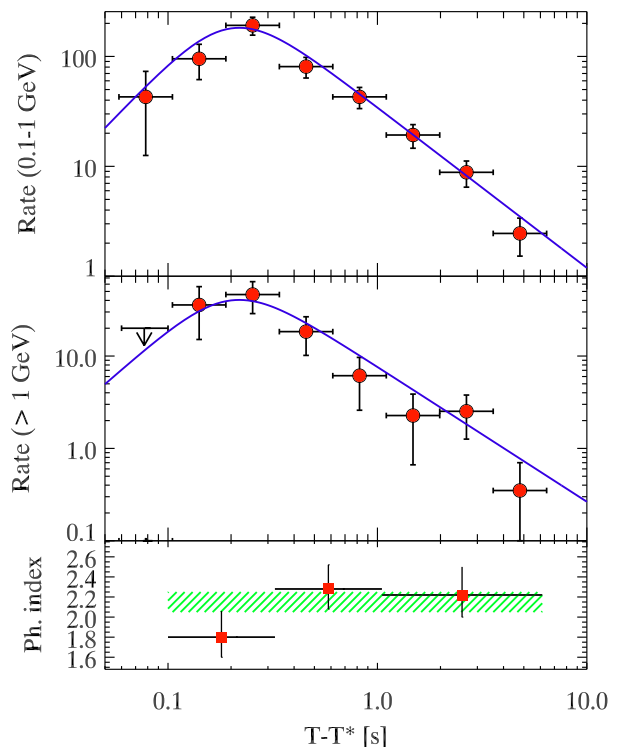


FIG. 2.— *Fermi*-LAT light curve of GRB 090510 between 0.1 and 1 GeV and above 1 GeV (top and middle panels, respectively) in the first 10 seconds. The times are scaled to $T^*=0.6$ s (see text). The solid line is the fit of the light curve >0.1 GeV (Fig. 1). The bottom panel shows the photon spectral index (1σ errors are shown) of the LAT spectra for the time-integrated spectrum (hatched region) and for three time-resolved spectra (squares).

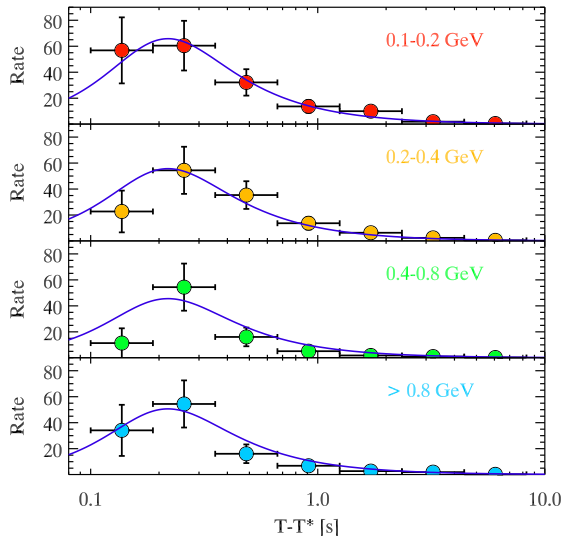


FIG. 3.— *Fermi*-LAT light curve of GRB 090510 in four energy channels (from top to bottom): 0.1–0.2 GeV, 0.2–0.4 GeV, 0.4–0.8 GeV, >0.8 GeV. The curves are the best fit obtained from the LAT light curve (>0.1 GeV - Fig. 1) rescaled to the single channel light curves.

0.8 GeV and >0.8 GeV (Fig. 3). Fig. 2 and Fig. 3 show that the time of the peak is the same in different energy ranges.

We also analyzed the spectra of the early GeV emission component. We considered the spectrum integrated in time between $T - T^* = 0.1$ and 7 s and we also extracted three time resolved spectra distributed in this time interval. The photon spectral index of the fit with a single power law of the average spectrum (hatched region) and of the time resolved spectra (filled squares) are shown in the bottom panel of Fig. 2. The spectrum before the peak is hard with a photon index 1.87 ± 0.2 and then it softens to 2.2 ± 0.2 . Both are consistent with the time-integrated spectrum.

4. ESTIMATE OF THE INITIAL BULK LORENTZ FACTOR

The derived peak time of the LAT received flux translates into an estimate of the bulk Lorentz factor Γ_0 at the start of the afterglow. The peak time of the afterglow bolometric luminosity occurs at a time of the order of the deceleration time. If the circumburst number density n is homogeneous we have (e.g. Sari & Piran 1999):

$$\frac{t_{\text{peak}}}{1+z} \sim t_{\text{dec}} \sim \left(\frac{3E_{\text{k,iso}}}{32\pi n m_p c^5 \Gamma_0^8} \right)^{1/3} \quad (2)$$

where $E_{\text{k,iso}}$ is the isotropic kinetic energy of the fireball, estimated through the emitted energy of the prompt emission assuming an efficiency η ($E_{\text{k,iso}} = E_{\gamma,\text{iso}}/\eta$). We use Eq. 2 to estimate Γ_0 . Setting $E_{\gamma,\text{iso}} = 3.5 \times 10^{52}$ erg (A09, excluding the LAT component), $\eta = 0.2$ and $t_{\text{peak}} = 0.2$ s we derive $\Gamma_0 = 1.96 \times 10^3 n^{-1/8}$. This value is not much larger than the lower limits derived by A09 through the compactness argument and assuming that the LAT component belongs to the prompt emission. It is also rather insensitive to the (unknown) particle density n . The distance from the central engine corresponding to the peak time is $R_{\text{peak}} \sim 2ct_{\text{peak}}\Gamma_0^2/(1+z) = 2.4 \times 10^{16} n^{-1/4}$ cm.

4.1. A synchrotron origin of the LAT emission

Following standard arguments, the minimum electron energy of the injected electrons in the forward shock is $\gamma_m \sim \epsilon_e \Gamma m_p / m_e$, while the magnetic field value is $B \sim \Gamma(8\pi\epsilon_B n m_p c^2)^{1/2}$. Electrons with γ_m emit an observed synchrotron frequency $\nu_m \sim 2\Gamma(4/3)eB/(2\pi m_e c)\gamma_m^2/(1+z) \sim 10.6\Gamma_3^4(n\epsilon_B)^{1/2}\epsilon_e^2/(1+z)$ MeV. This frequency is below the LAT energy range, but the injection of a power law distribution of electrons extending to $\gamma_{\text{max}} \sim (10^2 - 10^3)\gamma_m$ ensures that the LAT flux can indeed have a synchrotron origin. The synchrotron self-Compton (SSC) spectrum extends to much higher frequencies (e.g. Fan et al. 2008, Corsi et al. 2009), but becomes important only above $\nu_{\text{m,C}} \sim \gamma_m^2\nu_m$, i.e. above the TeV energy range. Note the strong dependence of ν_m and $\nu_{\text{m,C}}$ on the bulk Lorentz factor: a synchrotron origin of a \sim GeV afterglow is reasonable only for rather large Γ_0 , while the SSC flux becomes more important for smaller Γ_0 .

This has a simple and important consequence. Bursts with $\Gamma_0 \sim 100$ or smaller can produce high energy afterglow radiation through the SSC mechanism but *the onset time of their afterglows* will be large, in turn implying, for the same emitted energy, a lower luminosity (see also Kumar & Barniol Duran 2009). They are then more difficult to detect. The best candidates for a LAT detection are therefore bursts with large Γ_0 , because this ensures an early onset of the afterglow, implying large luminosities.

5. TEST OF THE LORENTZ-INVARIANCE VIOLATION

The arrival time of the 30 GeV photon coincides with the peak of the afterglow emission. This is reasonable, because this is the time when we have the maximum probability to detect it (maximum flux and hard spectrum). *If we assume* that the 30 GeV photon was indeed produced at the peak time, then the maximum possible time delay it can have is of the order of the width of the time bin of the peak (0.15 s). More conservatively, we can assume that the 30 GeV photon was produced right at the beginning of the afterglow and it arrives delayed by 0.22 s due to violation of the Lorentz invariance.

The time delay Δt between the arrival time of a low and a high energy photon in the case of a linear dependence of the photon's propagation speed on its energy is

$$\Delta t = \frac{\Delta E}{M_{\text{QG}}c^2} \int_0^z \frac{1+z}{H_0\sqrt{\Omega_m(1+z)^3 + \Omega_\Lambda}} dz \quad (3)$$

where ΔE is the difference between the low and high photon energy and M_{QG} is the quantum-gravity mass (A09; Amelino-Camelia et al. 1998; Jacob & Piran 2008).

For a delay of 0.15 s we derive $M_{\text{QG}} > 6.7M_{\text{Planck}}$ while the more conservative limit (delay of 0.217 s) is $M_{\text{QG}} > 4.7M_{\text{Planck}}$ (we used $h_0 = 0.71$, $\Omega_\Lambda = 0.73$, $\Omega_M = 0.27$). These limits are consistent with those of A09, but excludes their lowest estimates.

6. CONCLUSIONS

The detection of an early high energy emission in the GeV range inevitably flags a large bulk Lorentz factor Γ_0 : to avoid suppression of the GeV emission due to the $\gamma\text{-}\gamma \rightarrow e^\pm$ process if the high energy photons belong to

the prompt phase, or to have an early peak flux time if the emission belongs to the afterglow phase.

We have shown that the latter case is indeed favored (see also Gao et al. 2009), because we see the peak time of the emission in the LAT light-curve (as also seen in other GRBs in the infrared–optical band, see e.g. Molinari et al. 2007 for GRB 060418 and GRB 060607A). Furthermore, also the energy spectral index $F(\nu) \propto \nu^{-1}$ is very similar to the ones we see in the afterglow phase. A large Γ_0 , implying an early onset of the afterglow, means a large luminosity at the peak time (for equal emitted energy), and large typical frequencies. This makes synchrotron the most likely process for the LAT emission we see.

GRBs with smaller Γ_0 will have their prompt emission less blue-shifted, and it would be more difficult for them to reach the LAT energy range during their prompt phase. Their afterglows can, through the SSC process, but their afterglow peak time is longer, and so their fluxes are fainter (as $t_{\text{peak}}^{-1} \propto \Gamma_0^{8/3}$ if they emit, at the peak, the same amount of energy, see Eq. 2). A large Γ_0 , instead, means a large blue-shift for the photons of the prompt, an early onset of the afterglow, implying more flux at the peak, and finally larger intrinsic afterglow frequencies, allowing even the synchrotron photons of the afterglow to reach the LAT energy range. Therefore GRBs with large Γ_0 should be much more luminous in the LAT energy

range than the other GRBs (see also Kumar & Barniol Duran 2009).

The limits derived here on the quantum gravity mass scale are not very different from the ones derived by A09, but we could associate the GBM and the LAT fluxes to two different components. We can then argue that the high energy photons are *generated* at (slightly) later times than the photons detected by the GBM, and the delay of their *arrival* times is not entirely due to quantum gravity effects. Instead, since photons above 100 MeV belong to the same component they are the best tool to investigate quantum gravity effects.

This suggests a recipe for a robust test on the Lorentz invariance violation, possible with very *bright* and *short* bursts detected at high energies. A *short* duration of the prompt ensures that the fireball has a relatively narrow width, and in turn this should correspond to a well-defined afterglow peak. A *bright* flux ensures good photon statistics, enabling to measure more accurately possible delays as a function of photon energies.

This research was supported by PRIN–INAF 2009 and ASI I/088/06/ grants. G. Ghirlanda acknowledges the NORDITA program on Physics of relativistic flows. We thank F. Tavecchio and Y. Poutanen for helpful discussions.

REFERENCES

- Abdo A.A., Ackermann M., Ajello M., et al. 2009, Nat. subm., arXiv:0908.1832
 Abdo A.A., Ackermann M., Arimoto M. et al., 2009a, Sci., 323, 1688
 Amelino–Camelia G., Ellis J., Mavromatos N.E., Nanopoulos D.V., Sarkar S., 1998, Nature, 393, 763
 Corsi A., Guetta D., Piro L., 2009, A&A subm., arXiv:0905.1513
 Fan Y.–Z., Piran T., Narayan R. & Da–Ming W., 2008, MNRAS, 384
 Gao W.–H., Mao J., Xu D., Fan Y.–Z., 2009, arXiv:0908.3975
 Giuliani A., Fuschino F., Vianello G., et al. 2009, ApJL subm., arXiv:0908.3975
 Golenetskii S., Aptekar R., Mazets E., et al. 2009, GCN 9344
 Guiriec S., Connaughton V., Briggs M., et al. 2009, GCN 9336
 Hoversten E. A., Barthelmy S. D., Burrows D. N., et al. 2009, GCN 9331
 Jacob U. & Piran T., 2008, PhRvD, 78, Issue 12, id. 124010
 Kumar P. & Barniol Duran R., 2009, Nat, subm., arXiv:0905.2417
 Longo F., Moretti E., Barbiellini G., et al., 2009, GCN 9343
 Ohmori N., Noda K., Sonoda E., et al., 2009, GCN, 9355
 Molinari E., Vergani S.D., Malesani D. et al., 2007, A&A, 469, L13
 Piran T., 2005, RvMP, 76, 1143
 Rau A., McBreen S., Kruehler T. et al. 2009, GCN 9353
 Razzaque S., Dermer C. D. & Finke J. D., 2009, ApJ subm., arXiv:0908.0513
 Sari R. & Piran T., 1999, ApJ, 520, 641
 Zhang B. & Peer A., 2009, ApJ, 700, L65
 Zou Y.–C., Fan Y.–Z., Piran T., 2009, MNRAS, 396, 1163